

Homogeneity of Surface Sites in Supported Single-Site Metal Catalysts: Assessment with Band Widths of Metal Carbonyl Infrared Spectra

| Adam S. Hoffman^a; Chia-Yu Fang^{a,b}; and Bruce C. Gates^{a*}

^aDepartment of Chemical Engineering, University of California at Davis, Davis, California, 95616, USA

^bDepartment of Materials Science and Engineering, University of California at Davis, Davis, California, 95616, USA

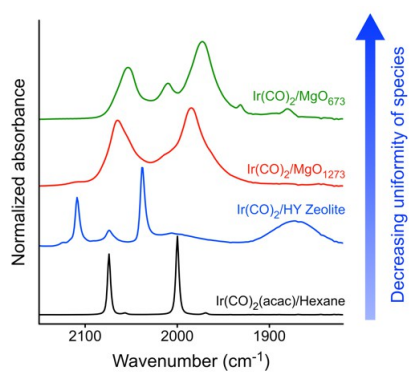
Corresponding Author

*Bruce C. Gates. Tel: (530) 752-3953 E-mail: bcgates@ucdavis.edu

ABSTRACT

~~Determining~~Identifying and controlling the uniformity of isolated metal sites on surfaces of supports are central goals in investigations of single-site catalysts, because well-defined species provide opportunities for fundamental understanding of the surface sites ~~for fundamental understanding and industrial applications~~. CO is a useful probe ~~molecule~~ of the surface metal sites, often reacting with them to form~~leading to the formation of~~ metal *gem*-dicarbonyls, the infrared spectra of which provide insights into the nature of the metal sites and the metal–support interface. Metals bonded to various~~to various~~ support surface sites give broad bands in the spectra, and when narrow Full width at half maximum values ~~characterizing the ν_{CO} values~~ bands are observed, they ~~provide evidence of~~ indicate a high the degree of uniformity of the metal sites; ~~because metals bonded to a set of various sites give broad bands in the spectra~~. Much recent work focused on single-site catalysts has been done with ~~uses~~ supports that are inherently non-uniform, giving supported metal species that are therefore leading to a non-uniform metal sites, ~~and ultimately resulting in a lack of fundamental understanding of the chemistry~~. Herein we summarize ~~new and already reported~~ values of ν_{CO} data characterizing supported iridium *gem*-dicarbonyls, showing that the most nearly uniform of them are those supported on zeolites and the least uniform ~~are~~ those supported on metal oxides. Guided by ν_{CO} data of supported iridium *gem*-dicarbonyls, we have determined new, general synthesis methods to maximize the degree of uniformity of iridium species~~ites~~ on zeolites and on MgO. ~~We that can be applied to other similar classes of support~~ report results for a zeolite HY-supported iridium *gem*-dicarbonyl with full width at half maximum values of only 4.62 and 5.23 cm^{-1} characterizing the symmetric and asymmetric CO stretches and implying that this is the most nearly uniform supported single-site metal catalyst.

TOC GRAPHIC



KEYWORDS

Single-site catalyst, infrared spectroscopy, metal *gem*-dicarbonyl, surface heterogeneity, iridium, rhodium

Single-site supported catalysts typically incorporate metal cations bonded to support oxygen atoms,^{1-2,3} and their catalytic properties depend markedly on the support.⁴⁻⁹ and activities compared to the supported metal clusters. Because almost all support surfaces are intrinsically heterogeneous, the supported species are nonuniform—bonded in various ways on various sites of the supports. Therefore, it is challenging to determine the structures of the supported species and the metal–support ~~bonding~~interaction bonding, and such information is incomplete in the above-mentioned work. The complexity of ~~such~~ these materials hinders fundamental understanding of their function as catalysts. ~~This complexity also gives rise to varied catalytic activity of the materials.~~ Physical characterization would provide the ~~deepest~~most understanding of these ~~sem~~ materials if the supports were ideal—~~that is,~~ perfectly crystalline ~~materials~~—with only single kinds of sites for bonding the metal. Herein we show how to assess the degree of uniformity of atomically dispersed metals on supports with infrared (IR) spectroscopy of CO ligands bonded to the metals, and ~~guided by the physical characterization data, we~~ report how ~~to~~ determined how to synthesize supported iridium complexes that ~~are evidently~~appear to be the most nearly uniform of any ~~single-site catalysts~~supported metal species. ~~Thus, this work demonstrates improved synthesis methods guided by the results and understanding of physical measurements.~~

Values of ν_{CO} characterizing a compound $\text{M}(\text{CO})_x\text{L}_y$, where M is a transition metal and L a ligand, with the subscripts x and y taking on ranges of values, are sensitive to the backbonding involving *d*-electrons of the metal and π^* orbitals of the CO ligands. ~~The~~Further, ν_{CO} values characterize the electron-donor properties of L as well as the symmetry of the compound.^{10-12, 4,5,6}

Further, the ν_{CO} values IR spectra similarly provide essential details of the local environments of metal sites on solid surfaces.⁷¹³

The typical mononuclear metal carbonyl complex on a metal oxide support is heterogeneous, characterized by a smear of species and broad ν_{CO} bands, but Miessner et al.⁸⁻¹⁴ showed that mononuclear rhodium carbonyls bonded to dealuminated HY zeolite are characterized by narrow ν_{CO} bands, indicating that the zeolite bonding sites are almost all the same. There are now numerous examples of single-site catalysts bonded to zeolites that broadly bear out Miessner's observations;^{3,159} some are listed in Table 1.

-Here we use full width at half maximum (FWHM) values of the carbonyl bands to classify supported metal complexes and show how this criterion can be used to guide helps to assess the synthesis to maximize the degree of uniformity of the of some of the most nearly uniform supported metal species. We report new synthesis methods demonstrating how to take advantage of optimizing (a) synthesis temperature, (b) the zeolite support Si/Al ratio, and (c) the degree of crystallinity and surface site uniformity of a metal oxide support, MgO, in order generate a higher, and in some cases, a nearly uniform supported Ir to maximize the degree of uniformity of supported iridium carbonyls.

Supported metal complexes were made from the precursor $\text{Ir}(\text{CO})_2(\text{acac})$ (acac is acetylacetonate, $\text{C}_5\text{H}_7\text{O}_2^-$) or $\text{Ir}(\text{C}_2\text{H}_4)_2(\text{acac})$ and zeolite or metal oxide supports by reaction of the precursor with support surface OH groups to give supported $\text{Ir}(\text{CO})_2$ ^{16-22,40-46} or $\text{Ir}(\text{C}_2\text{H}_4)_2$ groups; with the iridium metal loadings of the samples being with metal loadings of 1.0 wt% Ir.^{16-19,22,40-43,46} Supported $\text{Ir}(\text{C}_2\text{H}_4)_2$ groups are readily converted to $\text{Ir}(\text{CO})_2$ by reaction with CO .^{16-19,22 40-43,46} Mild (temperature and pressure no greater than 298 K and 1 bar, respectively)

synthesis and characterization conditions were used in order to prevent metal site aggregation that occurs at higher temperatures.²³

In the reported room-temperature synthesis with zeolite HY,^{18,21+2,15} Ir(CO)₂(acac), which is barely soluble in *n*-pentane, evidently dissolved in this solvent, ~~was is~~ transported to the zeolite, and reacted with zeolite OH groups. Syntheses with a wide range of supports have similarly given a family of supported Ir(CO)₂ complexes (Table 1), and a number of them have been characterized by extended X-ray absorption fine structure (EXAFS) data showing that each Ir atom (on average) bonds to 2 oxygen atoms of the support.^{18,21,22,24+2,15-17} IR data characterizing the CO ligands confirm the presence of anchored iridium *gem*-dicarbonyls,^{18,19,21,22,24+2,13,15-17} and DFT calculations²⁵⁺⁸ support the structure assignments.-

Now we report improved synthesis methods that give more nearly uniform supported species than those reported,

~~including We report FWHM values of the carbonyl bands to demonstrate the uniformity.~~

Because the precursor Ir(CO)₂(acac) does not dissolve visibly in *n*-pentane solvent at room temperature, we carried out a new synthesis~~some syntheses~~ at 193 K (the “low-temperature synthesis”) in the following way: a flask containing *n*-pentane, zeolite HY particles, and Ir(CO)₂(acac) crystals was placed in a dry ice/isopropanol bath, and, over 24 h, the initially white zeolite particles turned light pink (Figure 1), and there was no observed change in the liquid color. Then the flask was slowly (over 30 min) warmed to room temperature, and the zeolite color turned to white/light gray (Figure 1). IR spectra consist of bands at 2109 and 2038 cm⁻¹ (Figure 2) characterizing the symmetric and asymmetric stretching frequencies of terminal CO ligands, that with the frequencies matching those previously reported for single-site iridium carbonyls and; confirming the formation of a supported iridium *gem*-dicarbonyl. The lack of

observed ν_{CO} . Failure to identify bands at lower frequencies characteristic of bridging iridium carbonyls confirms the assignment to ~~we are confident in the single-site assignments~~ species. (The band characterizing the zeolite-supported sample and located between the iridium *gem*-dicarbonyl bands (Figure 2), at 2074 cm^{-1} , has been attributed to iridium tricarbonyl species, inferred, consistent with our weak bands, to be a minority species.²⁶) ~~Need Reason for Tricarbonyl... cannot come up with one...~~ The band observed at 1870 cm^{-1} observed in (Figure 2) for the $\text{Ir}(\text{CO})_2/\text{HY}$ zeolite is assigned to framework vibrations of the zeolite, and it is correspondingly present in the IR spectra of the support prior to ~~addition~~ the incorporation of the iridium.



Figure 1. Images characterizing samples at two stages of the low-temperature synthesis as $\text{Ir}(\text{CO})_2(\text{acac})$ reacted with zeolite HY to give a loading of 1.0 wt% Ir. Left: ~~a~~ After $\text{Ir}(\text{CO})_2(\text{acac})$ and zeolite HY had been slurried in *n*-pentane for 24 h in a dry ice bath at (193 K); right: after the slurry had been allowed to warm to 298 K in a period of approximately 30 min.

In a comparison experiment (the “~~room~~high-temperature synthesis,” matching that reported^{18,21,42,45}), the reactants and solvent were slurried at room temperature, and the zeolite turned light gray in color as the $\text{Ir}(\text{CO})_2(\text{acac})$ crystals dissolved and the precursor reacted with the zeolite. A comparison of the IR data characterizing the two samples (Table 1) shows that the frequencies of the CO bands characterizing the supported iridium *gem*-dicarbonyls were the same in both, with the symmetric stretch observed at 2109 cm^{-1} and the asymmetric stretch at

2038 cm^{-1} , but the FWHM results differ, with the values for the low-temperature synthesis being 4.6 and 5.2 cm^{-1} for ν_{sym} and ν_{asym} , respectively, and those for the roomhigh-temperature synthesis being 5.3 and 5.6 cm^{-1} , respectively. Errors in the This comparison shows that the new low-temperature synthesis method gives a more nearly uniform sample than the roomhigh-temperature method. Deviation in the FWHM values offor the ν_{sym} and ν_{asym} were found to be ± 0.2 and ± 0.4 cm^{-1} , respectively, determined from data characterizing based upon comparing 7seven separately madeunique batches of $\text{Ir}(\text{CO})_2/\text{zeolite HY}$. Thus, the comparison shows that the new low-temperature synthesis method gives more nearly uniform samples than the room-temperature method. These errors show that the difference in the FWHM observed between the room- and low-temperature syntheses are unique and that synthesis temperature does influences the uniformity of the metal sites. (The band characterizing the zeolite-supported sample and located between the iridium *gem*-dicarbonyl bands (Figure 2), at 2074 cm^{-1} , has been attributed to iridium tricarbonyl species.¹⁹)

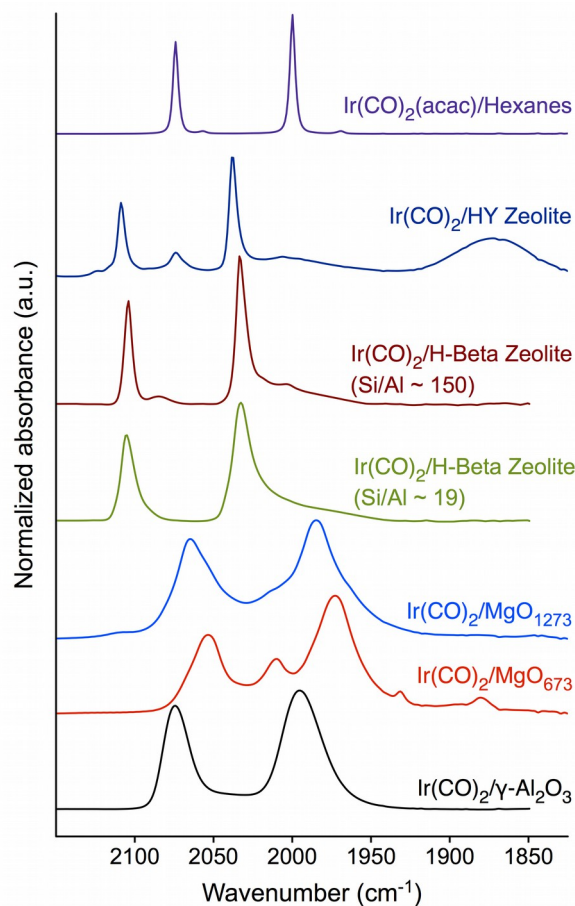


Figure 2. IR spectra in the ν_{CO} region of supported $\text{Ir}(\text{CO})_2$ complexes demonstrating the variation FWHM as the uniformity of the bonding sites on the support surfaces decreases, roughly from top to bottom. $\text{Ir}(\text{CO})_2$ on HY zeolite was made by the low-temperature method described in the text. The spectrum of $\text{Ir}(\text{CO})_2/\gamma\text{-Al}_2\text{O}_3$ is taken reproduced from the work of Lu et al.¹⁹

The results are consistent with the interpretation that the slow initial low-temperature adsorption of the precursor gave an initially nearly uniform distribution of iridium in the zeolite pores, followed by the higher-temperature reaction of the precursor with the zeolite surface to maintain such a distribution. We infer that in the low-temperature synthesis the precursor dissolved slowly in the *n*-pentane and diffused into the zeolite pores where it slowly became physisorbed before reacting, favoring an even distribution of metal in the zeolite and giving the pink sample with physisorbed precursor—and, when the temperature was later increased, these

species reacted with the zeolite surface OH groups, liberating acac ligands¹⁶⁻²²¹⁰⁻¹⁶ and turning the pink sample white with Ir(CO)₂ groups bonded to the zeolite. In contrast, we infer that in the room-high-temperature synthesis, the iridium complex reacted more quickly with the zeolite surface before it could spread evenly within the zeolite pores, thereby giving a less than uniform distribution of the iridium, which was likely concentrated near the pore mouths. Further investigation with electron microscopy would be able to sort out the difference in metal distribution between the two synthesis temperatures, comparing the Ir bonded to the edges/amorphous regions[ref Claudia acs catal 2014] and that in the pores, definitively determining if low temperature synthesis improves uniformity.



Figure 1. Images characterizing samples at two stages of synthesis as Ir(CO)₂(acac) reacted with zeolite HY to give a loading of 1.0 wt% Ir. Left: After Ir(CO)₂(acac) and zeolite HY had been slurried in *n*-pentane for 24 h in a dry ice bath (193 K); right: after the slurry had been allowed to warm to 298 K in approximately 30 min.

For comparison of the supported species with dissolved molecular species, we determined FWHM values for the CO bands of the pure precursor Ir(CO)₂(acac) dissolved in mixed hexanes; the values are 3.9 and 4.0 cm⁻¹ for the symmetric and asymmetric stretches at 2074 and 2000 cm⁻¹, respectively (Table 1, Figure 2); as best we can tell, these data match within error those already reported for Ir(CO)₂(acac) in hexane.²⁰²⁷ The satellite-weak bands at 2056 and 1967 cm⁻¹ have been assigned to-as natural-abundance ¹³CO stretching frequenciesbands.²⁰²¹

Most important for our work, the FWHM values of the dissolved iridium complex are only slightly less than those observed for the HY zeolite-supported sample made in the low-temperature synthesis (Figure 2) ~~compared to that in any other metal oxide~~. The bands characterizing this zeolite-supported iridium *gem*-dicarbonyl are as narrow as any reported for such a supported species, and, to our knowledge, are consistent with the ~~suggestion~~ *inference* that it is the most nearly uniform ~~such~~-supported *single-site catalyst sample*.

Reports of numerous other supported metal carbonyl complexes are characterized by much broader bands than these (Table 1, Figure 2). For example, an γ -Al₂O₃-supported iridium complex is characterized by FWHM values that are an order of magnitude greater than those of the zeolite-supported sample (Table 1).

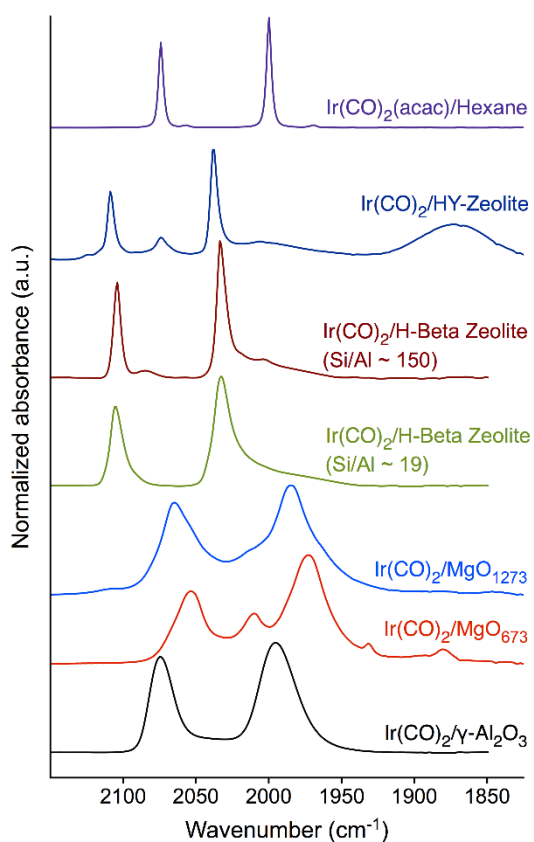


Figure 2. IR spectra in the ν_{CO} region of supported $\text{Ir}(\text{CO})_2$ complexes demonstrating the variation FWHM as the uniformity of the bonding sites on the support surfaces decrease, roughly from top to bottom. The $\text{Ir}(\text{CO})_2/\gamma\text{-Al}_2\text{O}_3$ is taken from the work of Lu et al.¹³

To test another strategy for increasing the degree of uniformity of supported iridium carbonyls, we carried out a similar synthesis with a different zeolite, H-Beta, again at 298 K, with $\text{Ir}(\text{CO})_2(\text{acac})$ as the precursor and the conditions stated above for the room-high-temperature synthesis. Two forms of zeolite H-Beta were used, one with a Si/Al atomic ratio of 19 and the other one with a Si/Al atomic ratio of 150. The IR data give evidence of nearly the same supported $\text{Ir}(\text{CO})_2$ groups in each of these zeolites, with the symmetric CO stretch observed at 2105 cm^{-1} and the asymmetric stretch at 2033 cm^{-1} , but, significantly, the FWHM values were found to be 5.4 and 7.4 cm^{-1} , respectively, for the sample with the sparse population of Al sites and 10.1 and 14.9 cm^{-1} , respectively, for the other (Table 1). We suggest that the zeolite with the more widely dispersed sites has a more nearly uniform set of such sites (Al-OH groups) for bonding to the iridium and therefore gives a more uniform set of iridium-containing species, or, alternatively, that the chemisorption of the precursor on the sparsely distributed sites takes place more slowly than on the less sparsely distributed sites, giving a more uniform distribution of the iridium before chemisorption takes place. The band near 2070 cm^{-1} corresponding to iridium tricarbonyl species was not observed in the zeolite beta samples. We speculate that the lack of band stems from zeolite beta having a higher degree of uniformity, whereas the pretreatment of zeolite Y generates amorphous regions adding non-uniformity to the sample.^{29ref} The lack of band near 2070 cm^{-1} indicated the presence of $\text{Ir}(\text{CO})_3$ species compared to the species observed in the HY zeolite. This absence is likely due to size exclusion due to the pore size of H-Beta (6.68 \AA) compared to HY (11.24 \AA) not allowing the formation of the tricarbonyl

We extended the synthesis method to a support with a much less uniform set of surface bonding sites than the zeolites, namely, MgO. The MgO samples were treated at various temperatures, 673, 1073, and 1273 K, under vacuum. These treatments lead to various degrees of bulk crystallinity, as shown by (a) differences in morphology observed by microscopy,²²³⁰ (b) variations in the OH sites on the surface inferred from IR²³³¹ and electron paramagnetic resonance spectra,²⁴³² and (c) DFT²⁵³³ models showing various surface structures and surface sites. Our treatment procedures gave samples of MgO that differed from each other in terms of (1) the average crystallite domain size, as determined by X-ray diffraction crystallography (XRD) (Figure 3), and (2) the surface hydroxyl group density, as shown in the Supporting Information.

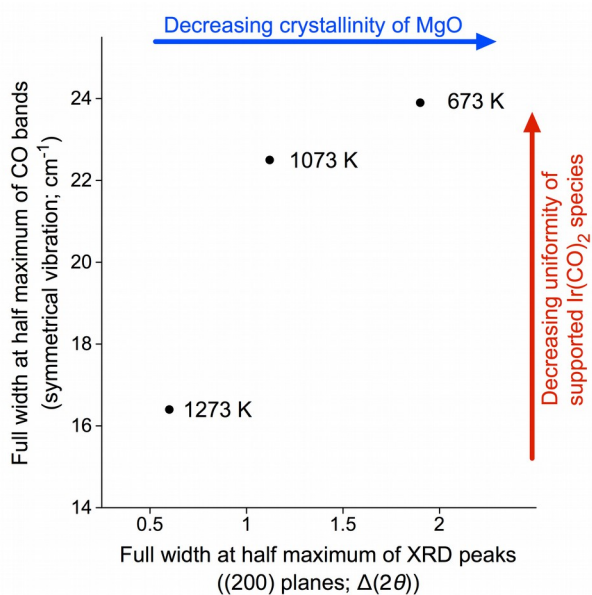


Figure 3. Correlation between the degree of crystallinity of the MgO support as measured by XRD and the degree of uniformity of the MgO-supported $\text{Ir}(\text{CO})_2$ complexes measured by the FWHM of the symmetric CO stretching band determined by IR spectroscopy. Temperatures next to the data points represent the pretreatment temperature of the MgO support.

The samples of MgO-supported $\text{Ir}(\text{CO})_2$, $\text{Ir}(\text{CO})_2/\text{MgO}_T$, where T is the MgO pretreatment temperature in K, were synthesized at 298 K by the roomhigh-temperature method mentioned

above, except that the precursor was $\text{Ir}(\text{C}_2\text{H}_4)_2(\text{acac})$. The synthesis gave supported $\text{Ir}(\text{C}_2\text{H}_4)_2$ species, as expected,^{16†9} and these were converted to $\text{Ir}(\text{CO})_2$ by treatment with CO, as expected before^{16†9} (Table 1). IR spectra show that the frequencies of the symmetric and asymmetric bands of the CO ligands depend on the MgO pretreatment temperature, T , consistent with the expectation that the surface bonding sites varied with T . Furthermore, the data demonstrate a decrease in the FWHM values of the ν_{CO} bands with increasing T (Figure 2 and Table 1), as follows: for the symmetric band, the FWHM started at 23.9 cm^{-1} and decreased to 22.5 cm^{-1} and then to 16.4 cm^{-1} as T increased from 673 to 1073 to 1273 K. A similar trend (FWHM values of 30.9, 30.4, and 15.5 cm^{-1} , respectively) was observed for the asymmetric stretch. Evidently the uniformity of the support bonding sites depends on the MgO pretreatment temperature, and the IR spectra demonstrate this point (although the structures of the bonding sites are still a matter of discussion).

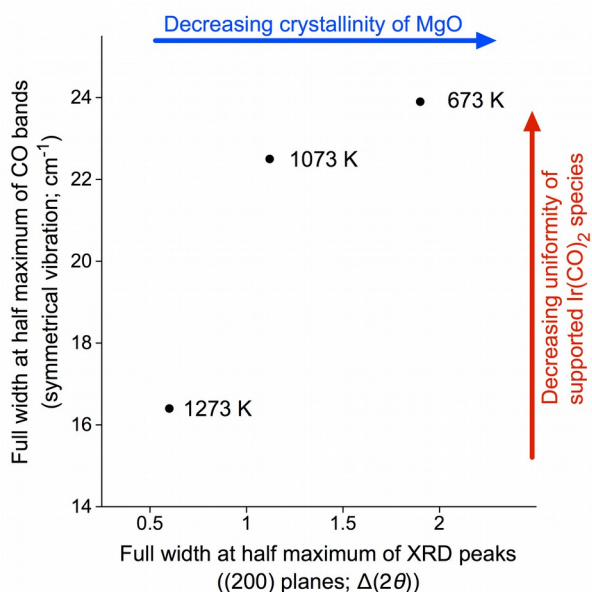


Figure 3. Correlation between the degree of crystallinity of the MgO support as measured by the FWHM of the MgO (200) plane determined by XRD measurements and the degree of uniformity of the MgO-supported $\text{Ir}(\text{CO})_2$ complexes measured by the FWHM of the symmetric

~~CO stretching band determined by IR spectroscopy. Temperatures next to the data points represent the pretreatment temperature of the MgO support.~~

The comparison shown in Table 1 of the FWHM values of the carbonyl bands in a family of supported Ir(CO)₂ complexes demonstrates a wide range of degrees of uniformity among the samples. Those having the highest degree in uniformity are zeolites, ~~with~~ metal organic frameworks (MOFs) ~~having~~ nodes that are small clusters of metal oxides ~~are~~ being less uniform than the zeolites, and bulk metal oxides ~~being~~ are even less uniform, with those having a highly crystalline character, illustrated by MgO, being more nearly uniform than less crystalline solids illustrated by γ -Al₂O₃. Figure 3 illustrates the results for a representative family of these materials.

In summary, we have illustrated several synthetic approaches to control the degree of uniformity of single-site supported metal catalysts, by varying (1) the synthesis temperature, (2) the zeolite Si/Al ratio, and (3) the degree of metal oxide crystallinity guided by physical characterization. The comparison of the FWHM values characterizing CO ligands on the iridium ~~in~~ a number of supported iridium carbonyls demonstrates a wide range of degrees of uniformity of the supported species and points to zeolites as the most nearly ideal reported supports for single-site catalysts with the low-temperature synthesis method giving most nearly uniform species reported—and these, we infer, provide some of the best opportunities for fundamental understanding of supported single-site metal catalysts.

Table 1. Comparison of supported single-site iridium and rhodium *gem*-dicarbonyl catalysts on the basis of the CO stretching frequencies and FWHM values, depending on the support and support treatment conditions, metal precursor, and synthesis conditions used to form the metal carbonyl.

Support	Support treatment	Precursor	Metal loading (wt %)	Synthesis conditions	ν_{CO} (cm ⁻¹)		Full width at half maximum of CO bands (cm ⁻¹)		Other characterization techniques	Reference
					Symmetric vibration	Asymmetric vibration	Symmetric vibration	Asymmetric vibration		
None (Ir(CO) ₂ (acac) in mixed hexanes)	--	Ir(CO) ₂ (acac)	--	--	2074	2000	3.9	4	--	This work
H-Beta zeolite (Si/Al ~ 19)	O ₂ 773 K 4 h; Vac. 773 K 16 h	Ir(CO) ₂ (acac)	1	Room temperature	2105 ^a	2033 ^a	10.1	14.9	--	This work
H-Beta zeolite (Si/Al ~ 150)	O ₂ 773 K 4 h; Vac. 773 K 16 h	Ir(CO) ₂ (acac)	1	Room temperature	2105 ^a	2033 ^a	5.4	7.4	--	This work
HY zeolite (Si/Al ~ 30)	O ₂ 773 K 2 h; Vac. 773 K 14 h	Ir(CO) ₂ (acac)	1	Room temperature	2109 ^a	2038 ^a	5.3	5.6	--	This work
HY zeolite (Si/Al ~ 30)	O ₂ 773 K 2 h; Vac. 773 K 14 h	Ir(CO) ₂ (acac)	1	Low- temperature Gold synthesis	2109 ^a	2038 ^a	4.6	5.2	--	This work
HY zeolite (Si/Al ~ 30)	O ₂ 773 K 2 h; Vac. 773 K 14 h	Ir(CO) ₂ (acac)	1	Room temperature	2109 ^a	2038 ^a	5	5	EXAFS spectroscopy; DFT calculation	2145
H-SSZ-42 zeolite (Si/Al ~ 15)	O ₂ 773 K 4 h; Vac. 773 K 16 h	Ir(C ₂ H ₄) ₂ (acac)	1	Room temperature; CO pulse	2102 ^a ; 2086 ^b	2029 ^a ; 2013 ^b	Broad	Broad	EXAFS spectroscopy	1943
H-SSZ-53 zeolite	O ₂ 723 K 1 h; Vac. 723 K 1 h	Ir(C ₂ H ₄) ₂ (acac)	1	Room temperature; CO pulse	2099 ^a	2027 ^a	10	10	EXAFS spectroscopy	1842
NaY zeolite (Si/Al ~ 2.6)	O ₂ 773 K 4 h; Vac. 773 K 12 h	Ir(CO) ₂ (acac)	1	Room temperature	2082 ^b	1995 ^b	Broad	Broad	EXAFS spectroscopy	2447

NU-1000	Vac. 363 K 2h; Vac. 393 K 12h	Ir(CO) ₂ (acac)	10	Room temperature	2066 ^a ; 2082 ^b	1990 ^a ; 2005 ^b	Broad	Broad	EXAFS spectroscopy; DFT calculation	2216
NU-1000	Vac. 363 K 2h; Vac. 393 K 12h	Ir(C ₂ H ₄) ₂ (acac)	1	Room temperature; CO pulse	2066 ^a	1900 ^a	Broad	Broad	EXAFS spectroscopy; DFT calculation	2216
UiO-66	Vac. 363 K 2h; Vac. 423 K 12h	Ir(CO) ₂ (acac)	10	Room temperature	2074 ^a ; 2085 ^b	1996 ^a ; 2010 ^b	Broad	Broad	EXAFS spectroscopy; DFT calculation	2216
UiO-66	Vac. 363 K 2h; Vac. 423 K 12h	Ir(C ₂ H ₄) ₂ (acac)	1	Room temperature; CO pulse	2074 ^a	1996 ^a	Broad	Broad	EXAFS spectroscopy; DFT calculation	2216
γ-Al ₂ O ₃	O ₂ 773 K 2 h; Vac. 773 K overnight	Ir(C ₂ H ₄) ₂ (acac)	1	Room temperature; CO pulse	2075 ^a	1996 ^a	30	30	EXAFS spectroscopy	1317
MgO	Vac. 523 K 75 min; 673 K 60 min	Ir(C ₂ H ₄) ₂ (acac)	1	Room temperature; CO pulse	2056 ^a	1973 ^a	23.9	30.9	--	This work
MgO	Vac. 523 K 75 min; 1073 K 60 min	Ir(C ₂ H ₄) ₂ (acac)	1	Room temperature; CO pulse	2061 ^a	1983 ^a	22.5	30.4	--	This work
MgO	Vac. 523 K 75 min; 1273 K 60 min	Ir(C ₂ H ₄) ₂ (acac)	1	Room temperature; CO pulse	2066 ^a	1985 ^a	16.4	15.5	--	This work
None (Rh(CO) ₂ (acac) in <i>n</i> -hexane)	--	Rh(CO) ₂ (acac)	--	--	2084	2015	2.8	2.9	--	2720
H-Beta zeolite (Si/Al ~ 19)	O ₂ 773 K 16 h; Vac. 773 K 4 h	Rh(CO) ₂ (acac)	1	Room temperature	2115 ^a	2048 ^a	9	9	EXAFS spectroscopy	2634
H-SSZ-42 zeolite (Si/Al ~ 15)	O ₂ 723 K 1 h; Vac. 723 K 1 h	Rh(CO) ₂ (acac)	1	Room temperature	2111 ^a ; 2082 ^b	2045 ^a ; 2020 ^b	Broad	Broad	EXAFS spectroscopy	3426
H-Mordenite ^e zeolite	O ₂ 773 K 16 h; Vac. 773 K 4 h	Rh(CO) ₂ (acac)	1	Room temperature	2111 ^a ; 2092 ^b	2045 ^a ; 2035 ^b	Broad	Broad	EXAFS spectroscopy	3426
HY zeolite (Si/Al ~ 30)	O ₂ 773 K 4 h; Vac. 773 K 16 h	Rh(C ₂ H ₄) ₂ (acac)	1	Room temperature; CO pulse	2117 ^a	2052 ^a	< 8	< 8	EXAFS spectroscopy; DFT calculation	3527
Ultra-stable Y zeolite (Si/Al ~ 95)	--	[Rh(NH ₃) ₅ Cl](OH) ₂	^c	^d	2118 ^a	2053 ^a	< 5	< 5	--	148

^a Assigned as chemisorbed species.

^b Assigned as physisorbed species.

^c The metal loading was not specified.

^d The synthesis was carried out by an ion-exchange method. Ultra-stable Y zeolite was mixed with $[\text{Rh}(\text{NH}_3)_5\text{Cl}](\text{OH})_2$ in an aqueous solution. The sample was dried at 383 K for 3 h and calcined in air at 673 K for 2 h. The calcined sample then reacted with CO (at 10 Torr and 423 K) for 30 min, followed by subsequent evacuation at 300 K.

EXPERIMENTAL METHODS

Syntheses. Room-temperature synthesis of Ir(CO)₂ on zeolite HY, H-Beta, or MgO ~~followed was done with~~ methods reported elsewhere.^{16-19,21,22,24,34,35 40-43,45-47,26,27} The supports were pretreated at temperatures from 773 to 1273 K in ~~an~~ O₂oxygen and/or under vacuum ~~atmosphere~~ to remove excess moisture and carbon--containing compounds. The precursor, Ir(CO)₂(acac) (Sigma-Aldrich) or Ir(C₂H₄)₂(acac) (synthesized in this work^{28,36}), and support ~~(~~HY zeolite (Zeolyst CBV 760), H-Beta zeolite (Zeolyst, CP814C and CP814C-300) or MgO (EMD)) were slurried in *n*-pentane (Sigma-Aldrich, 98%) then evacuated to remove the solvent. Low-temperature synthesis of Ir(CO)₂ on zeolite HY was achieved by placing a Schlenk flask containing the metal precursor, Ir(CO)₂(acac), zeolite powder, and *n*-pentane in a Dewar filled with a bath containing dry ice and isopropanol, with the slurry stirred for 24 h. The flask was then removed and allowed to warm to room temperature before the *n*-pentane was removed by evacuation. The air- and moisture-sensitive samples were stored in an argon-atmosphere glovebox. In an argon- atmosphere, tThe supported Ir(C₂H₄)₂ samples were packed in a flow reactor or flow-through cell, transferred to a flow system without exposure to air, and then--and exposed to CO (Airgas 10% in helium) to form the Ir(CO)₂ species. The carbonyl species were recovered in the glovebox.

IR spectroscopy. A Bruker IFS-66VS spectrometer was used to collect spectra of samples that had been loaded into an air-tight flow-through cell in an argon-atmosphere glovebox to minimize oxygen and moisture exposure. CO exchange was conducted as spectra were being recorded in-situ to monitor the conversion from the iridium diethylene to the iridium dicarbonyl complex. Each spectrum is an average of 64 scans collected over 2 min. Details of the experiments with solid samples are reported elsewhere.^{16-19,21,22,24,34,35} The spectrum of Ir(CO)₂(acac) in hexanes (EM

Science, 98.5%) was measured with a saturated solution in a sealed liquid IR cell (International Crystal Laboratories) with a 0.5--mm path length.

Associated Content

Supporting Information contains the IR spectra and XRD diffraction patterns of the MgO supports pretreated at various temperatures and EXAFS data characterizing a zeolite-supported iridium gem-dicarbonyl.

Corresponding Author

Corresponding Author: Bruce C. Gates. Tel: (530) 752-3953 E-mail: bcgates@ucdavis.edu

Acknowledgements

We acknowledge support from the U.S. Department of Energy (DOE), Office of Science (SC), Basic Energy Sciences (BES), Grant DE-FG02-04ER15513, and support of ASH by a Chevron Fellowship. We thank Dr. C. Y. Chen and colleagues at Chevron Energy Technology Company for helpful discussions and for performing the XRD experiments.

References

- (1) [\(1\)](#)Flytzani-Stephanopoulos, M. Gold Atoms Stabilized on Various Supports Catalyze the Water-Gas Shift Reaction. *Acc. Chem. Res.*, **2014**, 47, 783-792.
- (2) [\(2\)](#)Yang, X.-F.; Wang, A.; Qiao, B.; Li, J.; Liu, J.; Zhang, T. Single-Atom Catalysts: A New Frontier in Heterogeneous Catalysis, *Acc. Chem. Res.*, **2013**, 46, 1740-1748.
- (3) [\(3\)](#)Serna, P.; Gates, B. C. Molecular Metal Catalysts on Supports: Organometallic Chemistry Meets Surface Science. *Acc. Chem. Res.*, **2014**, 47, 2612-2620.

- (4) [Manna, K.; Ji, P.; Lin, Z.; Greene, F. X.; Urban, A.; Thacker, N. C.; Lin, W. Chemoselective Single-Site Earth-Abundant Metal Catalysts at Metal-Organic Framework Nodes. *Nature Communications*, **2016**, doi:10.1038/ncomms12610](#)
- (5) [Li, Z.; Schweitzer, N. M.; League, A. B.; Bernales, V.; Peters, A. W.; Getsoian, A. B.; Wang, T. C.; Miller, J. T.; Vjunov, A.; Fulton, J. L. et al. Sintering-Resistant Single-Site Nickel Catalyst Supported by Metal-Organic Framework. *J. Am. Chem. Soc.* **2016**, *138*, 1977-1982.](#)
- (6) [Mouat, A. R.; Lohr, T. L.; Wegener, E.; Miller, J.; Delferro, M.; Stair, P. C.; Marks, T. J. Reactivity of a Carbon-Supported Single-Site Dioxo-Molybdenum Catalyst for Biodiesel Synthesis. *ACS Catal.* **2016**, DOI: 10.1021/acscatal.6b01717](#)
- (7) [Romanenko, I.; Gajan, D.; Sayah, R.; Crozet, D.; Jeanneau, E.; Lucas, C.; Leroux, L.; Veyre, L.; Lesage, A.; Emsley, L. et al. Iridium\(I\)/N-Heterocyclic Carbene Hybrid Materials: Surface Stabilization of Low-Valent Iridium Species for High Catalytic Hydrogenation Performance. *Angew. Chem. Int. Ed.* **2015**, *54*, 12937-12941.](#)
- (8) [Duan, H.; Li, M.; Zhang, G.; Gallagher, J. R.; Huang, Z.; Sun, Y.; Luo, Z.; Chen, H.; Miller, J. T.; Zou, R.; Lei, A. et al. Single-Site Palladium\(II\) Catalyst for Oxidative Heck Reaction: Catalytic Performance and Kinetic Investigation. *ACS Catal.* **2015**, *5*, 3752-3759.](#)
- (9) [Matsubu, J. C.; Yang, V. N.; Christopher, P. Isolated Metal Active Site Concentration and Stability Control Catalytic CO₂ Reduction Selectivity. *J. Am. Chem. Soc.* **2015**, *137*, 3076-3084.](#)

- (10) [\(4\)](#)Cotton, F. A.; Wilkinson, G.; Murillo, C. A.; Bochmann, M. *Advanced Inorganic Chemistry*, 6th Edition; Wiley: New York, 1999.
- (11) [\(5\)](#)Nakamoto, K. *Infrared Spectra of Inorganic and Coordination Compounds*; Wiley-Interscience: New York, 1970.
- (12) [\(6\)](#)Braterman, P. S. *Metal Carbonyl Spectra*; Academic Press: Cambridge, 1975.
- (13) [\(7\)](#)Hadjiivanov, K. I.; Vayssilov, G. N. Characterization of Oxide Surfaces and Zeolites by Carbon Monoxide as an IR Probe Molecule. *Adv. Catal.*, **2002**, *47*, 307-511.
- (14) [\(8\)](#)Miessner, H.; Burkhardt, I.; Gutschick, D.; Zecchina, A.; Morterra, C.; Spoto, G. The Formation of a Well Defined Rhodium Dicarbonyl in Highly Dealuminated Rhodium-exchanged Zeolite Y by Interaction with CO. *J. Chem. Soc., Faraday Trans. 1*, **1989**, *85*, 2113-2126.
- (15) [\(9\)](#)Flytzani-Stephanopoulos, M.; Gates, B. C. Atomically Dispersed Supported Metal Catalysts. In *Annual Review of Chemical and Biomolecular Engineering*, Prausnitz, J. M.; Doherty, M. F.; Segalman, R. A., Eds.; Annual Reviews: Palo Alto, 2012; Vol. 3, 545-574.
- (16) [\(10\)](#)Lu, J.; Serna, P.; Gates, B. C. Zeolite- and MgO-Supported Molecular Iridium Complexes: Support and Ligand Effects in Catalysis of Ethylene Hydrogenation and H–D Exchange in the Conversion of H₂ + D₂. *ACS Catal.* **2011**, *1*, 1549-1561.
- (17) [\(11\)](#)Lu, J.; Serna, P.; Aydin, C.; Browning, N. D.; Gates, B. C. Supported Molecular Iridium Catalysts: Resolving Effects of Metal Nuclearity and Supports as Ligands. *J. Am. Chem. Soc.* **2011**, *133*, 16186-16195.

- (18) [\(12\)](#) Lu, J.; Aydin, C.; Liang, A. J.; Chen, C.-Y.; Browning, N. D.; Gates, B. C. Site-Isolated Molecular Iridium Complex Catalyst Supported in the 1-Dimensional Channels of Zeolite H-SSZ-53: Characterization by Spectroscopy and Aberration-Corrected Scanning Transmission Electron Microscopy. *ACS Catal.* **2012**, *2*, 1002-1012.
- (19) [\(13\)](#) Lu, J.; Aydin, C.; Browning, N. D.; Gates, B. C. Oxide- and Zeolite-Supported Isostructural Ir(C₂H₄)₂ Complexes: Molecular-Level Observations of Electronic Effects of Supports as Ligands. *Langmuir* **2012**, *28*, 12806-12815.
- (20) [\(14\)](#) Planas, N.; Mondloch, J. E.; Tussupbayev, S.; Borycz, J.; Gagliardi, L.; Hupp, J. T.; Farha, O. K.; Cramer, C. J. Defining the Proton Topology of the Zr₆-Based Metal-Organic Framework NU-1000. *J. Phys. Chem. Lett.* **2014**, *5*, 3716.
- (21) [\(15\)](#) Martinez-Macias, C.; Chen, M.; Dixon, D. A.; Gates, B. C. Single-Site Zeolite-Anchored Organoiridium Carbonyl Complexes: Characterization of Structure and Reactivity by Spectroscopy and Computational Chemistry. *Chem. Eur. J.* **2015**, *21*, 11825-11835.
- (22) [\(16\)](#) Yang, D.; Odoh, S. O.; Wang, T. C.; Farha, O. K.; Hupp, J. T.; Cramer, C. J.; Gagliardi, L.; Gates, B. C. Metal-organic Framework Nodes as Nearly Ideal Supports for Molecular Catalysts: NU-1000- and UiO-66-supported Iridium Complexes. *J. Am. Chem. Soc.* **2015**, *137*, 7391-7396.
- (23) [Bayram, E.; Lu, J.; Aydin, C.; Uzun, A.; Browning, N. D.; Gates, B. C.; Finke, R. G. Mononuclear Zeolite-supported Iridium: Kinetic, Spectroscopic, Electron Microscopic, and Size-Selective Poisoning Evidence for an Atomically Dispersed True Catalyst at 22 °C. ACS Catal. 2012, 2, 1947-1957.](#)

- (24) [\(17\)](#) Li, F.; Gates, B.C. Synthesis and Structural Characterization of Iridium Clusters Formed Inside and Outside the Pores of Zeolite NaY. *J. Phys. Chem. B.* **2003**, *107*, 11589-11596.
- (25) [\(18\)](#) Chen, M.; Serna, P.; Lu, J.; Gates, B. C.; Dixon, D. A. Molecular Models of Site-Isolated Cobalt, Rhodium, and Iridium Catalysts Supported on Zeolites: Ligand Bond Dissociation Energies. *Comp. Theor. Chem.* **2015**, *1074*, 58-72.
- (26) [\(19\)](#) Mihaylov, M.; Ivanova, E.; Thibault-Starzyk, F.; Daturi, M.; Dimitrov, L.; Hadjiivanov, K. New Types of Nonclassical Iridium Carbonyls Formed in Ir-ZSM-5: A Fourier Transform Infrared Spectroscopy Investigation. *J. Phys. Chem. B.* **2006**, *110*, 10383-10389.
- (27) [\(20\)](#) Dougherty, T. P.; Grubbs, W. T.; Heilweil, E. J. Photochemistry of Rh(CO)₂(acetylacetonate) and Related Metal Dicarbonyls Studied by Ultrafast Infrared Spectroscopy. *J. Phys. Chem.* **1994**, *98*, 9396-9399.
- (28) [\(21\)](#) Landmesser, H.; Burkhardt, I.; Miessner, H. Surface Carbonyl Species on Highly Dealuminated NaY Zeolite, an FT-IR investigation. Presented at the 8th International Conference on Fourier Transform Spectroscopy, Lübeck-Travemünde, Germany, September **1991**; 612, doi:10.1117/12.56398.
- (29) [Mañinez-Macias, C.; Xu, P.; Hwang, S.-J.; Lu, J.; Chen, C.-Y.; Browning, N. D.; Gates, B. C. Iridium Complexes and Clusters in Dealuminated Zeolite HY: Distribution between Crystalline and Impurity Amorphous Regions. *ACS Catal.* **2014**, *4*, 2662-2666.](#)

- (30) ~~(22)~~ Spoto, G.; Gribov, E. N.; Ricchiardi, G.; Damin, A.; Scarano, D.; Bordiga, S.; Lamberti, C.; Zecchina, A. Carbon Monoxide on MgO from Dispersed Solids to Single Crystals: A Review and New Advances. *Prog. Surf. Sci.* **2004**, *76*, 71-146.
- (31) ~~(23)~~ Knözinger, E.; Jacob, K.-H.; Singh, S.; Hofmann, P. Hydroxyl Groups as IR Active Surface Probes on MgO Crystallites. *Surf. Sci.* **1993**, *290*, 388-402.
- (32) ~~(24)~~ Chiesa, M.; Paganini, M. C.; Giamello, E.; Murphy, D. M.; Di Valentin, C.; Pacchioni, G. Excess Electrons Stabilized on Ionic Oxide Surfaces. *Acc. Chem. Res.* **2006**, *39*, 861-867.
- (33) ~~(25)~~ Chizallet, C.; Costentin, G.; Che, M.; Delbecq, F.; Saute, P.; Infrared Characterization of the Hydroxyl Groups on MgO: A Periodic and Cluster Density Functional Theory Study. *J. Am. Chem. Soc.* **2007**, *129*, 6442-6452.
- (34) ~~(26)~~ Ogino, I.; Chen, C.Y.; Gates, B.C. Zeolite-supported Metal Complexes of Rhodium and of Ruthenium: A General Synthesis Method Influenced by Molecular Sieving Effects. *Dalton Trans.* **2010**, *39*, 8423-8431.
- (35) ~~(27)~~ Liang, A. J.; Craciun, R.; Chen, M.; Kelly, T. G.; Kletnieks, P. W.; Haw, J. F.; Dixon, D. A.; Gates, B. C. Zeolite-Supported Organorhodium Fragments: Essentially Molecular Surface Chemistry Elucidated with Spectroscopy and Theory. *J. Am. Chem. Soc.* **2009**, *131*, 8460-8473.
- (36) ~~(28)~~ Bhirud, V. A.; Uzun, A.; Kletnieks, P. W.; Craciun, R.; Haw, J. F.; Dixon, D. A.; Olmstead, M. M.; Gates, B. C. Synthesis and Crystal Structure of Ir(C₂H₄)₂(C₅H₇O₂). *J. Organomet. Chem.* **2007**, *692*, 2107-2133.